Proceedings of the ASME 2022 International Design Engineering Technical Conferences & Computers and Information in Engineering Conference
IDETC/CIE 2022
August 14-17, 2022, St. Louis, Missouri

IDETC2022-89621

HARNESSING OPERATIONAL FLEXIBILITY FROM POWER TO HYDROGEN IN A GRID-TIED INTEGRATED ENERGY SYSTEM

Jubeyer Rahman*
The University of Texas at Dallas
Richardson, TX 75080
Email: jubeyer.rahman@utdallas.edu

Roshni Anna Jacob*
The University of Texas at Dallas
Richardson, TX 75080
Email: roshni.jacob@utdallas.edu

Jie Zhang†
The University of Texas at Dallas
Richardson, TX 75080
Email: jiezhang@utdallas.edu

ABSTRACT

Integrated energy systems (IES) are desirable in the power system due to their self-sufficiency and prompt response during critical operating conditions. In addition to reinforcing the system robustness, they are also capable of providing a number of ancillary services. Over the recent years, clean hydrogen has been explored as a promising solution to help the operation of a low-carbon grid. This work seeks to evaluate the benefits of integrating a hydrogen production facility into an IES infrastructure from the perspective of operation flexibility. Specifically, a grid-connected IES that consists of a small modular reactor (SMR), a wind farm, an electrolyzer that produces hydrogen, a fuel cell that converts hydrogen to electricity, and a hydrogen storage tank, is modeled and studied. The IES components are modeled considering their suitability for performing both power system unit commitment and economic dispatch simulations, and in this study we focus on day-ahead simulations. The proposed IES configuration aims to leverage the low-cost surplus generation (from SMR or wind) to produce hydrogen that could be used in peak load periods or traded in the hydrogen market. The results on the NREL 118-bus system simulation show that the IES could help reduce the total production cost and renewable curtailment in the system operation.

Keywords: Power to hydrogen, wind curtailment, integrated energy system, low-temperature electrolysis, small modular reactor.

1 Introduction

An Integrated Energy System (IES) is a hybrid power plant that is used for both electricity and heat, which could couple nuclear, renewable, and other energy sources. IES is expected to be deployed rapidly due to their energy independence, economic competitiveness, and optimal use of resources. Such units provide a lucrative path to energy austerity, aiming to save some of the 40% energy that is wasted worldwide in the electricity generation process [1]. The optimal co-ordination among different energy carriers within the IES could significantly increase the efficiency of the system. With the proliferation of Power-to-X technology, IES is being studied comprehensively for its role in providing different services [2], such as industrial heating, desalination, fertilizer production, hydrogen generation [3], district cooling, etc. Hydrogen is perceived as one of the most promising alternatives for storing surplus energy. Consequently, the use of hydrogen facilities is rapidly increasing along with an unprecedented growth in research interest on hydrogen generation process. Hydrogen facilities can function either as dispatchable power sources or interruptible loads, thus making hydrogen a good fit in a power grid with high renewable

*Ph.D. Student, Department of Electrical and Computer Engineering.

†Associate Professor, Department of Mechanical Engineering, Department of Electrical and Computer Engineering (Affiliated), and Center for Wind Energy (Affiliated), ASME Professional Member. Address all correspondence to this author.

penetration. Hydrogen could help offer the desired flexibility to tackle the ever-increasing challenges that come with the widespread installation of variable renewable resources. These hydrogen facilities can hence accommodate the renewable generation which would otherwise be curtailed in the absence of enough headroom during the generation-load balancing paradigm [4, 5].

There exist several processes to produce hydrogen such as the steam-methane reformation [6], methanol steam reformation [7], water electrolysis [8], etc. The most mature method for large-scale hydrogen production is the electrolytic hydrogen technology [9], due to its simple and efficient process without involving any moving parts. The available electrolytic technologies mostly differ from each other by type of electrolyte used in the chemical environment, which in turn affects the cost, efficiency, and energy consumption. Since this study mainly focuses on reaping the benefits of hydrogen for energy markets, the mode of energy available to produce hydrogen is a key factor in choosing the technology for study. Low-temperature electrolysis technologies are preferred due to their comparatively lower energy requirement [10]. Among the available electrolytic technologies, three of them are prominent: i) the proton exchange membrane (PEM) water electrolysis, ii) the alkaline water electrolysis, and iii) the solid oxide electrolysis. Each of the three technologies has its own pros and cons. The alkaline water electrolysis technology is cheaper, more matured, and more durable but is disregarded in applications where high hydrogen gas purity and current densities are required [11]. Solid oxide electrolysis occurs in a solid oxide medium and offers a competitive performance only at high temperature electrolysis, which requires additional provision of thermal energy [12]. Compared to the other two technologies, the PEM water electrolysis technology has advantages such as producing purer hydrogen gas, having remarkably higher current densities (upto 3 A/cm^2 (commercially) 10 A/cm^2 (in laboratory)), starting faster [13], and being compact. Thus for high power applications, PEM water electrolysis is preferred despite its comparatively higher capital cost.

Though a significant amount of work has been performed on the process of hydrogen generation from different energy sources, studies from the operational perspective in terms of energy scheduling, dispatch, and electricity markets are either less-detailed or overly simplified. For example, Ban et al. [14] proposed a day-ahead security constrained unit commitment (DASCUC) model for a grid-tied energy hub which offers power-to-hydrogen (P2H) and hydrogen-to-power (H2P) service from a wind-dominant site. Ye and Yuan [15] formulated a mixed-integer linear programming (MILP) model for exploring the operational characteristics of a grid-connected integrated electricity-heat-hydrogen system. In the MILP formulation, the system operation framework is modeled with only a few system-level constraints (e.g., load balance, transmission, and generator ramping). The study in Ref. [3] investigated the optimal operation strategy of a grid-connected wind-electrolytic hydrogen generation facility, while again adopting a simplified MILP model that disregards many important constraints (e.g., generator reserves, commitment number, etc.). Pan et al. [16] performed an operational study on an electricity-hydrogen IES that considers both power-to-hydrogen and power-to-heat applications with a seasonal hydrogen storage model. Li et al. [17] has performed a year-long techno-economic study on producing hydrogen from a wind farm while considering given electricity market prices. Song et al. [18] studied a two-stage stochastic scheduling model of an integrated electricity and natural gas system, where the flexible ramping constraints along with the spinning reserve requirement were considered while neglecting the impact of the IES on the electricity market. Liu et al. [13] proposed a coupled electricity-hydrogen market model and compared the benefit of the hydrogen facility within a microgrid. In Ref. [19], a day-ahead scheduling framework was developed as a mixed integer non-linear programming (MINLP) model to find the optimal operation schedule for a hybrid system with a hydrogen generating facility and a combined heat and power plant. A number of studies [20, 21, 22, 23] have also investigated the effectiveness and feasibility of producing hydrogen from nuclear-based IES.

1.1 Research Objective

Nuclear and renewable energy sources are important to consider in the U.S. economy's evolution because both are clean, non-carbon-emitting energy sources. Green hydrogen produced using nuclear and renewable electricity could play an important role in a clean energy future. While nuclear-renewable-hydrogen IES is being evaluated for their economic/environmental benefits and technical feasibility, most of existing works in the literature have not integrated hydrogen in large-scale power system networks to comprehensively evaluate the benefits of hydrogen at utility scale while considering the whole system operational constraints.

This study attempts to model the hydrogen generation in a large-scale power system operation framework, and explore the use of nuclear-renewable-hydrogen IES in both energy markets and ancillary service markets. Specifically, this study aims to evaluate the benefits of co-generation in facilitating load-following capability of less flexible plants like nuclear.

The main contributions of this study are twofold: (i) We develop a model to produce clean hydrogen from nuclear and allow hydrogen to participate in electricity mar-

kets. The developed nuclear-wind-hydrogen IES model is connected to a power transmission network and simulated with an energy scheduling and electricity market simulation tool [24]. (ii) Instead of taking historical price signals as inputs like most of the existing IES studies, our modeled nuclear-wind-hydrogen IES plays a price-maker role and can impact the electricity market signals, which is more realistic in power system operations.

The remainder of the paper is organized as follows. The power system optimization framework and the models of each component in the IES are described in Section 2. Section 3 describes the experimental setup for studying IES in electricity markets. The case study results are discussed in Section 4. Concluding remarks and future work are discussed Section 5.

2 Integrated Energy System Modeling

The proposed grid-connected nuclear-wind-hydrogen IES, as shown in Fig. 1, is comprised of the following components: (i) a pressurized water small modular reactor (SMR) of 320 MW_e, (ii) a wind plant of 149.5 MW_e, (iii) an electrolyzer of 30 MW_e, (iv) a fuel cell of 30 MW_e, and (v) a hydrogen storage tank of 1000 kg.

Detailed descriptions regarding the steady-state models developed for each of these components are provided in the following subsections. For the sake of brevity, only the constraint formulations relevant to the newly developed components of IES are described here. More detailed constraints formulation for the SMR and the electrical system can be found in our previous work [25].

2.1 Day-ahead Security Constrained Unit Commitment (DASCUC) Model

In the DASCUC model, the objective of the IES operation is to maximize the revenue which is formulated in Eq. 1 as the cost to be deducted from the system operation cost.

$$\begin{aligned} \boldsymbol{min} \sum_{t\in T}\Bigg[\sum_{g\in G\setminus G_{IES}}(su_{g,t}+sd_{g,t}+pc_{g,t}+\sum_{r\in RS}rc_{g,t,r})+ls_t\Bigg] \\ +\sum_{t\in T}\sum_{r\in RS}VOIR_r ir_{t,r}-\Bigg[\sum_{t\in T}\sum_{g\in G_{IES}}(\sum_{r\in RS}rc_{g,t,r})+pc_{g,t}\Bigg] \end{aligned} \tag{1}$$

Here, T denotes the set of the time interval, G is the set of the generators, RS is the set of reserve types, and G_{IES} is the set of the IES generators. The parameter $su_{g,t}$ represents the startup cost of generator g at time t, $sd_{g,t}$ denotes the shutdown cost, and $pc_{g,t}$ stands for the production cost. Since the DASCUC model used in this study considers the reserve provision as a part of ancillary services, those reserves are also reflected in the objective function. Four types of reserves are considered, which are the regulation reserve, spinning reserve, non-spinning reserve, and replacement reserve. The term $rc_{g,t,r}$ represents the cost associated with the procurement of reserve r. To minimize the reserve insufficiency, a penalty term $VOIR_r$ (i.e., value of insufficient reserve) is also included to be paid for the amount of reserve insufficiency of magnitude $ir_{t,r}$. The parameter ls_t stands for the cost associated with the load-shed by the system due to resource deficit. The reserve and production cost incurred by the IES generators (i.e., nuclear, wind, and fuel cell) are maximized as a negative part of the minimization problem. As a part of the model development, system level constraints such as power balance constraints, reserve

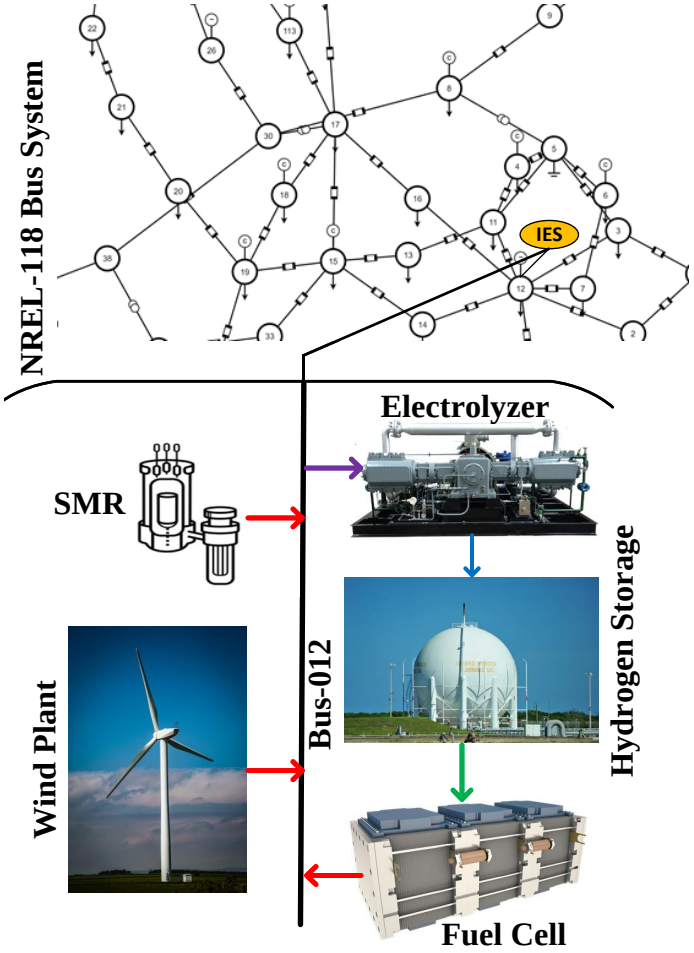

FIGURE 1: The nuclear-wind-hydrogen IES that is connected to a transmission network.

balance constraints, net injection, load flow, and branch limit constraints are considered. Among the machine level constraints, the generator's minimum capacity limit constraints, maximum capacity limit constraints, ramp-down constraints, ramp-up constraints, commitment constraints, reserve capability constraints, and constraints related to reserve limitations when in start-up and shut-down mode are considered.

For the IES export maximization purpose, the bus-wise net energy constraint has been modified to accommodate the net export from the IES. The system level constraints which are explicitly modified to accommodate the IES are described as follows:

$$p_{b,t}^{net} = \sum_{g \in G \setminus G_{IES}} p_{b,g,t} IF_{b,g} - D_{b,t} + \delta_{b,t} + \begin{cases} \sum_{g \in G_{IES}} p_{b,g,t}, & \forall b \in B_{IES}, \forall t \in T \\ 0, & \text{otherwise} \end{cases} \quad (2)$$

$$lf_{l,t} = \sum_{b \in B} PTDF_{l,b} p_{b,t}^{net}, \forall l \in L, \forall t \in T \quad (3)$$

Eq. 2 represents the bus-wise net energy injection constraint. Here, the term $p_{b,t}^{net}$ represents the net power inject at bus b at the t^{th} interval, $p_{b,g,t}$ stands for the power output of unit g at bus b at time t, $IF_{b,g}$ denotes the injection factor of unit g at bus b, $D_{b,t}$ is the electrical demand at bus b at time t, and $\delta_{b,t}$ is the shed load at that bus at time t. This cumulative power injection accommodates additional injection at the IES buses (B_{IES}) where applicable. Line flows are calculated by using the power transfer distribution factor (PTDF) matrix in Eq. 3, which is also modified to reflect the impact of the inclusion of IES to the system. Here, $lf_{l,t}$ stands for the line flow in line l at time t, and $PTDF_{l,b}$ represents the PTDF from bus b to line l.

2.2 Electrolyzer

An electrolyzer converts electrical energy to chemical energy in the form of hydrogen. Although the efficiency of an electrolyzer varies with the output, in this study a constant efficiency has been assumed for simplicity. Since the current study is performed in the steady-state domain, the slower dynamics of the electrolyzer is not considered. It has been reported that the output of the electrolyzer depends on the temperature, which is not considered in this study. Some essential parameters for the modeled electrolyzer are summarized in Table 1, and these parameter specifications are standardized and scaled based on the work in Ref. [26].

Constraints regarding the electrolyzer model are described as follows:

TABLE 1: Parameters of the electrolyzer

Parameter	Value
Maximum input electric power	30 MW
Ramp rate	10.5 MW/min
Minimum up & down time	1 hr
Start-up & shut-down time	15 min
Energy demand for H_2 production	55 kwh/kg

$$D_{EZ}^{min} \leq D_{EZ}^{t} \leq D_{EZ}^{max} \quad (4)$$

$$D_{EZ}^{t} - D_{EZ}^{t-1} \leq R_{EZ}^{UP} \cdot \Delta t \quad (5)$$

$$D_{EZ}^{t-1} - D_{EZ}^{t} \leq R_{EZ}^{LO} \cdot \Delta t \quad (6)$$

where D_{EZ}^{t} is the electrical power demand of the electrolyzer at time t, which is constrained between the minimum demand D_{EZ}^{min} and the maximum demand D_{EZ}^{max}. At any moment t, the electrolyzer demand is also restricted by its ramp-up rate R_{EZ}^{UP} and ramp-down rate R_{EZ}^{LO}, compared to its previous or following timestamp demand as described in Eqs. 5 & 6, respectively.

2.3 Small Modular Pressurized Water Reactor

A small modular pressurized water reactor is selected as the primary source of reliable power supply in the IES. To satisfy the purpose of steady-state analysis, constraints corresponding to the SMR modeling are kept similar to a conventional steam power plant, while the operating parameters are chosen to comply with the operational characteristics of the SMR from the literature [27, 28, 29, 30, 31] and scaled according to the specifications under this study. Some of the key machine specific constraints that define the operating characteristics of the developed SMR model are described below.

$$\overline{p}_{g,t} - \sum_{r \in RS} rr_{g,t,r} \leq p_{g,t-1} + R_g^U v_{g,t-1} + R_g^{SU}[v_{g,t} - v_{g,t-1}] + P_g^{max}(1 - v_{g,t}), \quad \forall g \in G, \forall t \in T, \forall r \in RS \quad (7)$$

$$\overline{p}_{g,t} \leq R_g^{SD}[v_{g,t} - v_{g,t+1}] + P_g^{max} v_{g,t+1}, \quad \forall g \in G, \forall t = 1, ..., |T| - 1 \quad (8)$$

$$p_{g,t} + \sum_{r \in RS} rr_{g,t,r} \leq \overline{p}_{g,t}, \forall g \in G, \forall t \in T, \forall r \in RS \quad (9)$$

Eqs. 7 - 9 enforce the satisfaction of reserve requirement while respecting the ramp limits of the SMR. Specifically, Eq. 7 ensures that the power output from the generating units does not violate the ramp-up limit both in normal operating hours and at the starting hours. Here, $\overline{p}_{g,t}$ represents the available output power of the SMR at time t, $rr_{g,t,r}$ is the amount of reserve of type r from unit g at time t, $p_{g,t-1}$ is the power output of the unit at the previous interval, R_g^U is the ramp-up limit for the unit g, R_g^{SU} denotes the ramp-up limit at the start-up interval, $v_{g,t}$ is the unit status at time t, and P_g^{max} stands for the maximum power output of unit g. Eq. 8 ensures that the ramp-down limit is respected at the shut-down hours. Here, R_g^{SD} represents the ramp-down limit for unit g at shutdown. Eq. 9 ensures that the generation does not surpass the available power output at a particular hour while also providing available reserves.

2.4 Fuel Cell

Fuel cells are used to convert chemical energy to electrical energy, and a utility scale fuel cell plant is adopted in this study to capitalize on the high electricity price at peak-load periods. The fuel cell model is conceived as a battery that can only discharge based on its state of charge. The adopted fuel cells are expected to convert the hydrogen back to electricity when the electricity price is high, since the optimization aims to maximize the revenue of the IES while reducing the overall system operation cost.

There are a number of fuel cells available in the literature, and the polymer exchange membrane fuel cell is chosen in this work, due to its higher efficiency, faster response, lower ohmic losses, and lower costs. Fuel cells are significantly slow in their dynamic responses but those delays are neglected in this steady-state analysis. Instead, some of the operational parameters that might be affected by the delayed responses are taken into consideration with proper parameter settings while developing the models. The steady-state model parameters that are affected by the delayed responses include ramp rate, minimum up & down time, start-up and shut-down time, which are summarized in Table 2 after proper scaling.

The active constraints that control the fuel cell's operational behavior are given below.

$$P_{FC}^{min} \leq P_{FC}^{t} \leq P_{FC}^{max} \quad (10)$$

$$P_{FC}^{t} - P_{FC}^{t-1} \leq R_{FC}^{UP} \cdot \Delta t \quad (11)$$

TABLE 2: Parameters of the fuel cell

Parameter	Value
Maximum output electric power	30 MW
Ramp rate	5 MW/min
Minimum up & down time	20 min
Start-up & shut-down time	15 min
Energy production rate	33 kwh/kg H_2 [32]

$$P_{FC}^{t-1} - P_{FC}^{t} \leq R_{FC}^{LO} \cdot \Delta t \quad (12)$$

$$(T_{UP}^{t-1} - MUT) \geq 0 \quad (13)$$

$$(T_{LO}^{t-1} - MDT) \geq 0 \quad (14)$$

Eq. 10 enforces the fuel cell generation P_{FC}^t within its maximum P_{FC}^{max} and minimum capacity P_{FC}^{min} at a particular time period. The ramping of the fuel cell to the next timestamp is constrained by its ramp-up rate R_{FC}^{UP} in Eq. 11; the ramping of the fuel cell from the previous timestamp is constrained by its ramp-down rate R_{FC}^{LO} in Eq. 12. Similar to the electrolyzer, the minimum up MUT and down time MDT are enforced here by Eqs. 13 & 14, respectively. Here T_{UP}^{t-1} represents the time duration when the fuel cell remains continuously on, and T_{LO}^{t-1} represents the time duration when the fuel cell remains continuously off.

2.5 Hydrogen Storage

When modeling the hydrogen storage system for the current study, the stored hydrogen is envisioned as accumulated electrical energy. Thus, the stored hydrogen amount or quantity is calculated as an equivalent amount of the electrolyzer consumption minus the fuel cell generation. Certain scaling factors are used for the conversions. Unlike other forms of storage where a balance constraint is enforced over the assumed optimization horizon, the initial hydrogen storage level is not bound to be equal to the final storage level at the end of the optimization period. Since it is an operational study, the storage cost is not included in the system operation cost, rather it should be considered in planning studies. Based on the optimization objective, i.e., maximizing the IES revenue while minimizing the operational cost of the whole system, the electrolyzer is expected to consume electricity to generate hydrogen when the electricity price is low and the fuel cell is expected to generate electricity from hydrogen when the electricity price is high.

So, the hydrogen storage is supposed to get charged at off-peak hours and discharged at peak hours of the day. While hydrogen can be stored in solid, liquid, or gaseous form, in order to keep the energy consumption low, it is assumed to be stored in the gaseous form in this study while admitting to the fact that storing hydrogen gas will require more investment in the hydrogen storage.

3 Experimental Setup

To quantify the benefits from adding hydrogen facility in the integrated energy system, a test network with high penetration of renewable, i.e., the NREL-118 bus system [33], is selected in our case study. There are 17 wind farms (4.38% installed capacity share) and 75 PV plants (14% installed capacity share) in the system. Determining the optimal location and size of the IES is a multi-year planning task, which is beyond the scope of this study. Instead, an empirical approach is adopted to determine a suitable placement location for the IES along with the hydrogen facility. Bus-12 is found to be the most suitable location to deploy the IES, since the particular interconnection creates less convergence issues. The IES components were connected to different load centers and the day-long simulation results were compared in terms of the overall production cost where bus-12 turned out to be the most suitable location for accommodating the proposed IES. The sizes of the IES components are also chosen empirically while also being realistic. The grid-tied IES is simulated on the DASCUC framework (in the Flexible Energy Scheduling Tool for Integrating Variable Generation (FESTIV) [24]) for one full day (January 1st, 2024) at hourly intervals. The modeling and optimization are performed in the GAMS (32.2)-based interface of FESTIV, whereas some of the system-level constraints of the DASCUC model are also modified to accommodate the IES components. The ILOG CPLEX 12.8 is adopted as the solver of the optimization model. All the renewable generation forecasts and plant specifications are collected from the NREL-118 bus system's database. Since the simulation is computationally intensive, a high performance computing system (i.e., Ganymede [34]) of 40-processors and 64 GB memory hosted at the University of Texas at Dallas was used for the simulation and one full-day simulation took approximately 2 minutes.

4 Results and Discussion

To better realize the operational benefits of the hydrogen generation facility, two cases are considered: i) the grid-tied IES is simulated without the hydrogen generation facility, and ii) the IES is simulated with the hydrogen facility. Figure 2 illustrates the hourly dispatch profiles of both the electrolyzer and the fuel cell. Since the objective is to maximize the revenue of the IES, the system attempts to generate hydrogen when the electricity price is low and consume hydrogen when the electricity price is high. It is validated from Fig. 2 that the electrolyzer generates hydrogen at the early hours of the day when the overall system demand as well as the electricity price are lower, whereas the hydrogen-based fuel cell generates power during the morning and evening peak load hours with higher electricity prices.

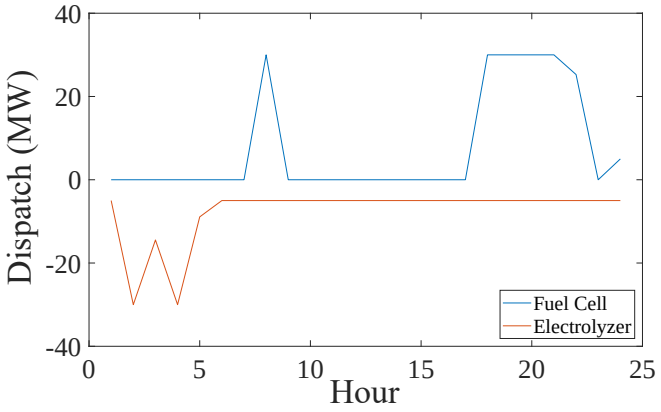

FIGURE 2: The hourly dispatch profiles of the deployed electrolyzer and fuel cell in the IES that is connected to the NREL-118 bus test system.

Since the optimization strategy tries to maximize the IES revenue, the operation of the hydrogen facility impacts the locational marginal price (LMP) of the IES node. Since the LMP determined from the DASCUC model is used to clear the market, higher prices will convince the IES to feed more power to the grid. It is observed from Fig. 3 that the operation of hydrogen facility increases the LMP at peak hours whereas it reduces the LMP at some off-peak hours. Due to the fairly small hydrogen capacity compared to the whole NREL-118 bus system, the impact on the LMP is not significant. More significant impacts are expected when increasing the number and capacity of electrolyzers.

Figure 4 shows the hourly storage profile of the hydrogen tank. It is seen that the storage gets charged at off-peak hours and discharged at peak hours, and the operational benefits are highly dependent on the hydrogen inventory. As mentioned that unlike other works where the storage is scheduled to have a daily operation strategy, this work focuses on studying the impact of hydrogen over a longer operation period, thus long-duration simulations will be required to comprehensively study the storage characteristics.

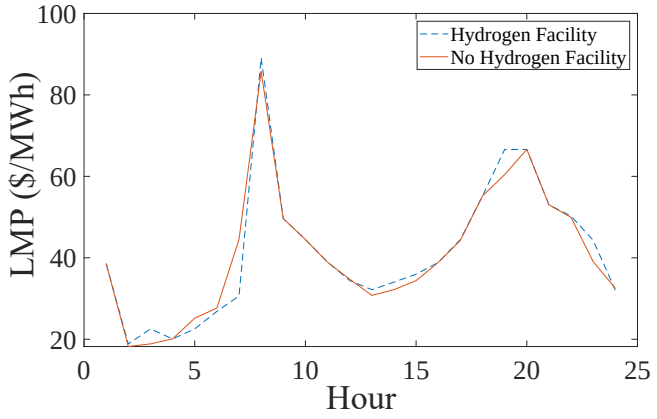

FIGURE 3: LMP comparison with and without the hydrogen generating facility

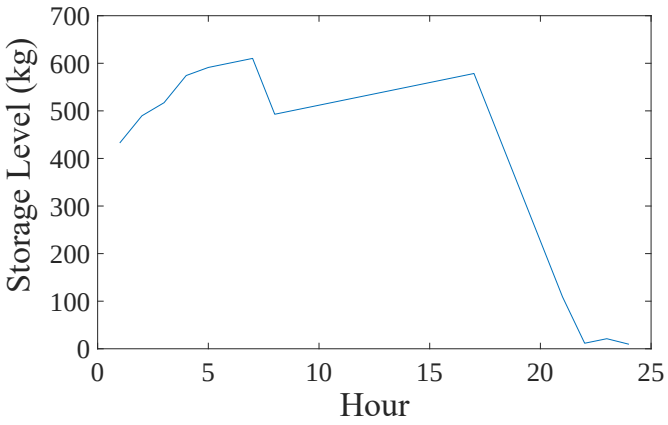

FIGURE 4: Hourly hydrogen storage profile.

Fig. 5 shows the renewable energy curtailment profile at the IES site. Without the hydrogen facility, a significant amount of wind energy is curtailed at the hours of wind abundance due to low load demand or transmission congestion. The curtailment has been drastically reduced after the deployment of the hydrogen facility in the IES. It is important to note that the curtailment is highly dependent on the capacity of the renewable generation, hydrogen facility, and the location of the IES, since the dispatch is subject to transmission capacity. Table 3 compares the system production cost (investment costs or depreciation costs have been excluded) and wind curtailment between the two cases (i.e., with or without hydrogen in the IES). It is seen that the addition of the hydrogen facility in the IES also helps reduce the overall production cost, since more renewable power is used for hydrogen production, which would otherwise be curtailed.

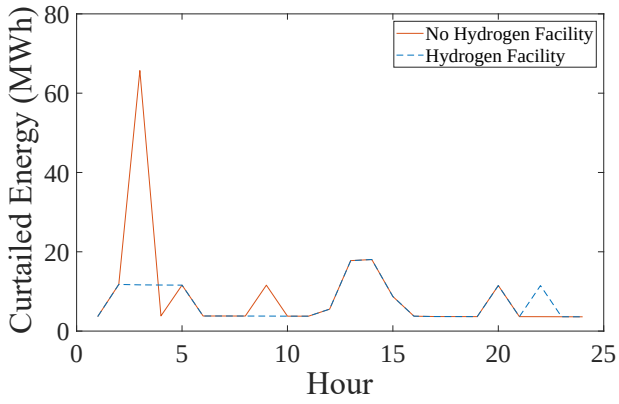

FIGURE 5: The curtailed renewable energy profile comparison: with and without the hydrogen facility in the IES.

TABLE 3: Production cost and curtailment comparison

Case	Production Cost ($)	Curtailment (MWh)
Without H_2 facility	6.3644×10^6	217.8193
With H_2 facility	6.3487×10^6	171.6204
Change (Δ)	**-15,700**	**-46**

5 Conclusion

This work investigated the operational flexibility harnessed from the addition of a hydrogen generation and storage facility to a grid-tied integrated nuclear and wind energy system. The dispatch of the IES components was determined via a day-long simulation with a day-ahead security constrained unit commitment model. The dispatch of fuel cell and electrolyzer were optimized in order to maximize the revenue of the IES. We found that the hydrogen facility could impact both the locational marginal price and renewable energy curtailment at the IES site.

Potential future work will (i) consider the xenon poisoning effect [35] in the modeling of the small modular reactor, and (ii) extend both the simulation timescale (from day-ahead to real-time dispatch) and horizon (from a single day to week-long simulations).

ACKNOWLEDGMENT

This material is based upon work supported by the the U.S. Department of Energy under Award No. DE-NE0008899.

REFERENCES

[1] INL. Integrated energy systems. [Online] Available at: https://ies.inl.gov/SitePages/Home.

[2] Abeysekera, M., Jenkins, N., and Wu, J., 2016. Integrated energy systems: An overview of benefits, analysis, research gaps and opportunities. Tech. rep., Hubnet Position Paper Series, Cardiff University, UK.

[3] Xiao, P., Hu, W., Xu, X., Liu, W., Huang, Q., and Chen, Z., 2020. "Optimal operation of a wind-electrolytic hydrogen storage system in the electricity/hydrogen markets". *International Journal of Hydrogen Energy,* ***45***(46), pp. 24412–24423.

[4] Badakhshan, S., Senemmar, S., Li, H., and Zhang, J., 2022. "Integrating offshore wind farms with unmanned hydrogen and battery ships". In *IEEE Kansas Power and Energy Conference (KPEC)*, Manhattan, Kansas, April 25-26, IEEE, pp. 1–6.

[5] Li, B., Sedzro, K., Fang, X., Hodge, B.-M., and Zhang, J., 2020. "A clustering-based scenario generation framework for power market simulation with wind integration". *Journal of Renewable and Sustainable Energy,* ***12***(3), p. 036301.

[6] Bakey, K., 2015. "The production of hydrogen gas: steam methane reforming". *ENGL 202C—Process Description*.

[7] Iulianelli, A., Ribeirinha, P., Mendes, A., and Basile, A., 2014. "Methanol steam reforming for hydrogen generation via conventional and membrane reactors: a review". *Renewable and Sustainable Energy Reviews,* ***29***, pp. 355–368.

[8] Nikolaidis, P., and Poullikkas, A., 2017. "A comparative overview of hydrogen production processes". *Renewable and sustainable energy reviews,* ***67***, pp. 597–611.

[9] Langmi, H. W., and Bessarabov, D. "Advanced hydrogen technologies for fc applications and pgm beneficiation in sa: Presentation". *HySA Catalysis and ZBT Workshop, Cape Town, SA, March 11-13, 2013*.

[10] Obodo, K. O., Ouma, C. N. M., and Bessarabov, D., 2021. "Low-temperature water electrolysis". In *Power to Fuel*. Elsevier, pp. 17–50.

[11] Weekly, M. Low-temperature water electrolysis trending for hydrogen production. [Online] Available at: https://www.miningweekly.com/article/low-temperature-water-electrolysis-trending-for-hydrogen-production-2020-09-18.

[12] Hauch, A., Jensen, S. H., Ramousse, S., and Mogensen, M., 2006. "Performance and durability of solid oxide electrolysis cells". *Journal of the Electrochemical Society,* ***153***(9), p. A1741.

[13] Liu, H., Wang, Y., Xu, F., Wu, M., Jiang, K., Yan, X., and Liu, N. "P2h modelling and operation in the microgrid under coupled electricity-hydrogen markets". *Frontiers in Energy Research*, p. 876.

[14] Ban, M., Yu, J., Shahidehpour, M., and Yao, Y., 2017. "Integration of power-to-hydrogen in day-ahead security-constrained unit commitment with high wind penetration". *Journal of Modern Power Systems and Clean Energy,* ***5***(3), pp. 337–349.

[15] Ye, J., and Yuan, R., 2018. "Stochastic scheduling of integrated electricity-heat-hydrogen systems considering power-to-hydrogen and wind power". *Journal of Renewable and Sustainable Energy,* ***10***(2), p. 024104.

[16] Pan, G., Gu, W., Lu, Y., Qiu, H., Lu, S., and Yao, S., 2020. "Optimal planning for electricity-hydrogen integrated energy system considering power to hydrogen and heat and seasonal storage". *IEEE Transactions on Sustainable Energy,* ***11***(4), pp. 2662–2676.

[17] Li, H., Rahman, J., and Zhang, J., 2022. "Optimal planning of co-located wind farm and hydrogen plant: A techno-economic analysis". In *The Science of Making Torque from Wind*, Delft, Netherlands, June 1-3, pp. 1–6.

[18] Song, X., Lin, C., Zhang, R., Jiang, T., and Chen, H., 2020. "Two-stage stochastic scheduling of integrated electricity and natural gas systems considering ramping costs with power-to-gas storage and wind power". *Frontiers in Energy Research,* ***8***, p. 289.

[19] Amin, M., Nazari-Heris, M., Mohammadi, B., and Marzband, M., 2019. "Day-ahead network-constrained scheduling of chp and wind based energy systems integrated with hydrogen storage technology". In 2019 27th Iranian Conference on Electrical Engineering (ICEE), IEEE, pp. 846–851.

[20] Orhan, M. F., and Babu, B. S., 2015. "Investigation of an integrated hydrogen production system based on nuclear and renewable energy sources: Comparative evaluation of hydrogen production options with a regenerative fuel cell system". *Energy,* ***88***, pp. 801–820.

[21] Orhan, M. F., Dincer, I., Rosen, M. A., and Kanoglu, M., 2012. "Integrated hydrogen production options based on renewable and nuclear energy sources". *Renewable and Sustainable Energy Reviews,* ***16***(8), pp. 6059–6082.

[22] Forsberg, C., 2005. "Futures for hydrogen produced using nuclear energy". *Progress in Nuclear Energy,* ***47***(1-4), pp. 484–495.

[23] Taljan, G., Cañizares, C., Fowler, M., and Verbic, G.,

2008. "The feasibility of hydrogen storage for mixed wind-nuclear power plants". *IEEE Transactions on Power Systems,* ***23***(3), pp. 1507–1518.

[24] Ela, E., Palmintier, B., Krad, I., et al., 2019. Festiv (flexible energy scheduling tool for integrating variable generation). Tech. rep., National Renewable Energy Lab.(NREL), Golden, CO (United States).

[25] Rahman, J., and Zhang, J., 2021. "Optimization of nuclear-renewable hybrid energy system operation in forward electricity market". In 2021 IEEE Green Technologies Conference (GreenTech), IEEE, pp. 462–468.

[26] Rouholamini, M., and Mohammadian, M., 2015. "Energy management of a grid-tied residential-scale hybrid renewable generation system incorporating fuel cell and electrolyzer". *Energy and Buildings,* ***102***, pp. 406–416.

[27] Poudel, B., and Gokaraju, R., 2021. "Optimal operation of smr-res hybrid energy system for electricity & district heating". *IEEE Transactions on Energy Conversion,* ***36***(4), pp. 3146–3155.

[28] Poudel, B., and Gokaraju, R., 2021. "Small modular reactor (smr) based hybrid energy system for electricity & district heating". *IEEE Transactions on Energy Conversion,* ***36***(4), pp. 2794–2802.

[29] Bose, D., Hazra, A., Mukhopadhyay, S., and Gupta, A., 2020. "A co-ordinated control methodology for rapid load-following operation of a pressurized water reactor based small modular reactor". *Nuclear Engineering and Design,* ***367***, p. 110748.

[30] Bose, D., Banerjee, S., Kumar, M., Marathe, P., Mukhopadhyay, S., and Gupta, A., 2017. "An interval approach to nonlinear controller design for load-following operation of a small modular pressurized water reactor". *IEEE Transactions on Nuclear Science,* ***64***(9), pp. 2474–2488.

[31] Jacob, R. A., Rahman, J., and Zhang, J., 2021. "Dynamic modeling and simulation of integrated energy systems with nuclear, renewable, and district heating". In *2021 North American Power Symposium (NAPS)*, IEEE, pp. 1–6.

[32] DOE. Fuel cells. [Online] Available at: `https://www.energy.gov/sites/prod/files/2015/11/f27/fcto_fuel_cells_fact_sheet.pdf`. Fuel Cell Technologies Office, Nov. 2015.

[33] Pena, I., Martinez-Anido, C. B., and Hodge, B.-M., 2017. "An extended ieee 118-bus test system with high renewable penetration". *IEEE Transactions on Power Systems,* ***33***(1), pp. 281–289.

[34] Ganymede-user-guide. [Online] Available at: `http://docs.oithpc.utdallas.edu/`. [Accessed: 2 March, 2020].

[35] Jenkins, J. D., Zhou, Z., Ponciroli, R., Vilim, R., Ganda, F., de Sisternes, F., and Botterud, A., 2018. "The benefits of nuclear flexibility in power system operations with renewable energy". *Applied energy,* ***222***, pp. 872–884.